THE JOURNAL OF BIOLOGICAL CHEMISTRY VOL. 291, NO. 30, pp. 15663–15673, July 22, 2016

Characterization of C-terminal Splice Variants of $Ca_v1.4$ Ca^{2+} Channels in Human Retina*

Received for publication, April 8, 2016, and in revised form, May 9, 2016 Published, JBC Papers in Press, May 17, 2016, DOI 10.1074/jbc.M116.731737

Françoise Haeseleer[‡], Brittany Williams[§¶], and Amy Lee[§‖1]**

*From the [‡]Department of Physiology and Biophysics, University of Washington, Seattle, Washington 98195 and the Departments of [§]Molecular Physiology and Biophysics, [‖]Otolaryngology Head-Neck Surgery, **Neurology, and [¶]Interdisciplinary Graduate Program in Neuroscience, University of Iowa, Iowa City, Iowa 52242*

Voltage-gated Ca^{2+} channels (Ca_v) undergo extensive alternative splicing that greatly enhances their functional diversity in excitable cells. Here, we characterized novel splice variants of the cytoplasmic C-terminal domain of $Ca_v1.4$ Ca^{2+} channels that regulate neurotransmitter release in photoreceptors in the retina. These variants lack a portion of exon 45 and/or the entire exon 47 ($Ca_v1.4\Delta$ex p45, $Ca_v1.4\Delta$ex 47, $Ca_v1.4\Delta$ex p45,47) and are expressed in the retina of primates but not mice. Although the electrophysiological properties of $Ca_v1.4\Delta$ex p45 are similar to those of full-length channels ($Ca_v1.4_{FL}$), skipping of exon 47 dramatically alters $Ca_v1.4$ function. Deletion of exon 47 removes part of a C-terminal automodulatory domain (CTM) previously shown to suppress Ca^{2+}-dependent inactivation (CDI) and to cause a positive shift in the voltage dependence of channel activation. Exon 47 is crucial for these effects of the CTM because variants lacking this exon show intense CDI and activate at more hyperpolarized voltages than $Ca_v1.4_{FL}$. The robust CDI of $Ca_v1.4\Delta$ex 47 is suppressed by CaBP4, a regulator of $Ca_v1.4$ channels in photoreceptors. Although CaBP4 enhances activation of $Ca_v1.4_{FL}$, $Ca_v1.4\Delta$ex 47 shows similar voltage-dependent activation in the presence and absence of CaBP4. We conclude that exon 47 encodes structural determinants that regulate CDI and voltage-dependent activation of $Ca_v1.4$, and is necessary for modulation of channel activation by CaBP4.

In the retina, voltage-gated $Ca_v1.4$ (L-type) Ca^{2+} channels are localized in the synaptic terminals of rod and cone photoreceptors where they mediate Ca^{2+} signals that trigger glutamate release at the first synapse in the visual pathway (1). In mice lacking expression of $Ca_v1.4$, there is a complete loss of photoreceptor synaptic transmission and a failure in photoreceptor synapse maturation (2–6). The importance of $Ca_v1.4$ for vision in humans is illustrated by the disorders associated with mutations in the *CACNA1F* gene encoding the pore-forming α_1 subunit of $Ca_v1.4$. These include congenital stationary night blindness type 2 (CSNB2 (7)),[2] X-linked cone-rod dystrophy (8, 9), and Åland island eye disease (10).

Compared with $Ca_v1.2$ channels that are prominent in the brain and heart, $Ca_v1.4$ channels activate at more negative voltages, and show very little inactivation during sustained depolarizations (11–13). It is thought that these properties support tonic glutamate release at the membrane potential of photoreceptors in darkness (−30 to −40 mV (14, 15)). Unlike other Ca_v channels, $Ca_v1.4$ does not undergo Ca^{2+}-dependent inactivation (CDI) (11–13)), a negative feedback regulation by incoming Ca^{2+} ions. For Ca_v1 and Ca_v2 channels, CDI is mediated by calmodulin (CaM) binding to site(s) in the proximal C-terminal domain of the pore-forming α_1 subunit (reviewed in Refs. 16 and 17)). In $Ca_v1.4$, a sequence in the distal C-terminal domain (C-terminal automodulatory domain, CTM) suppresses CDI through an intramolecular interaction with the proximal C-terminal domain (18–20). In addition to effects on CDI, the CTM inhibits voltage-dependent activation of $Ca_v1.4$. A CSNB2-causing mutation deletes the CTM from $Ca_v1.4$ (K1591X (21)), unmasks strong CDI, and causes a hyperpolarizing shift in the voltage dependence of activation (22), both of which would be expected to decrease the dynamic range of photoreceptor signal transmission (15).

Like other Ca_v channels, $Ca_v1.4$ undergoes alternative splicing that can greatly alter the functional properties of the channel. For example, a splice variant that removes a large fraction of the C-terminal domain including the CTM ($Ca_v1.4$ ex43*) is expressed in human retina and exhibits robust CDI and hyperpolarized activation voltages in transfected HEK-293 cells (23). Such properties, as in K1591X (22), might be expected to cause pathological changes in visual signaling. However, photoreceptors in the retina express CaBP4, a member of a family of Ca^{2+}-binding proteins (CaBPs) related to CaM (24). CaBP family members prevent CDI of Ca_v1 channels (25–27), in part by competing with CaM for binding sites on the channel (28–30). CaBP4 binds to the C-terminal domain of $Ca_v1.4$ channels containing the CTM, and enhances voltage-dependent activation. CaBP4 does not affect CDI, which is already nullified in full-length $Ca_v1.4$ channels (31, 32). Coexpression of CaBP4 with $Ca_v1.4$ channels lacking the CTM strongly suppresses CDI as in full-length channels (32). Therefore, splice variants lacking the

* This work was supported by National Institutes of Health Grants EY020850 (to F. H.), NS084190 and DC009433 (to A. L.), and a Carver Research Program of Excellence Award (to A. L.). The content is solely the responsibility of the authors and does not necessarily represent the official views of the National Institutes of Health. The authors declare that they have no conflicts of interest with the contents of this article.

[1] To whom correspondence should be addressed: Dept. of Molecular Physiology and Biophysics, Otolaryngology Head-Neck Surgery and Neurology, 169 Newton Rd., PBDB 5318, Iowa City, IA 52242. Tel.: 319-384-1762; Fax: 319-335-7330; E-mail: amy-lee@uiowa.edu.

[2] The abbreviations used are: CSNB2, congenital stationary night blindness type 2; CDI, Ca^{2+}-dependent inactivation; CTM, C-terminal automodulatory domain; CaM, calmodulin; CaBP, Ca^{2+}-binding protein; CT, C terminal domain; aa, amino acid; qPCR, quantitative PCR; ANOVA, analysis of variance; FL, full-length.

TABLE 1
Sequences of primers used for PCR

	Variant/species	Forward primer	Location forward	Reverse primer	Location reverse
1	$Ca_v1.4_{FL}$	5′-GAGGAAGTCCCTGATCGGCTTTC-3′	Ex44/45 jct	5′-CCCTCTGAGATAAGCACAGCCTC-3′	Ex47/48 jct
2	$Ca_v1.4$ Δex p45,47/ human	5′-GAAGTCCCTGATCGAGCTCAGAGA-3′	Ex44/pex45 joint	5′-CTCTGAGATAAGCACCTGAGCCC-3′	Ex46/48 joint
3	$Ca_v1.4_{FL}$/monkey	5′-GAGGAAGTCCCTGATCGGCTCTC-3′	Ex44/45 jct	5′-CCCTCCGATATGAGCACAGCCTC-3′	Ex47/48 jct
4	$Ca_v1.4$ Δex p45,47/ monkey	5′-GAAGTCCCTGATCGAGCTCAGAGA-3′	Ex44/pex45 joint	5′-CTCCGATATGAGCACCTGAGCCC-3′	Ex46/48 joint
5	$Ca_v1.4_{FL}$/mouse	5′-CAGGAACTCCCTGACTGGACTCC-3′	Ex44/45 jct	5′-CCTTCGGAGATGAGCACAGCCTC-3′	Ex47/48 jct
6	$Ca_v1.4$ Δex p45,47/ mouse	5′-GAACTCCCTGACTGGGTCCAGCAA-3′	Ex44/pex45 joint	5′-TTCGGAGATGAGCACCTGAGCCC-3′	Ex46/48 joint
7	$Ca_v1.4$ Δex p45/ human	5′-GAAGTCCCTGATCGAGCTCAGAGA-3′	Ex44/pex45 joint	5′-CAGGCACGTGCAGACAGGTGAA-3′	Ex47
8	$Ca_v1.4$ Δex p47/ human	5′-CCCTGATCGGCTTTCCTACCTAGATGA-3′	Ex45	5′-CTCTGAGATAAGCACCTGAGCCC-3′	Ex46/48 joint
9	$Ca_v1.4_{FL}$/human	5′-CCCTGATCGGCTTTCCTACCTAGATGA-3′	Ex45	5′-CAGGCACGTGCAGACAGGTGAA-3′	Ex47
10	GAPDH/human	5′-TCAACGGATTTGGTCGTATTGGGC-3′		5′-AGTGATGGCATGGACTGTGGTCAT-3′	
11	GAPDH/monkey	5′-TCAACGGATTTGGTCGTATTGGGC-3′		5′-AGTGATGGCGTGGACTGTGGTCAT-3′	
12	GAPDH/mouse	5′-GAAGGGCTAATGACCACAGTCCAT-3′		5′-TAGCCATATTCGTTGTCGTACCAGG-3′	

CTM may exhibit properties consistent with native photoreceptor Ca_v channels (*i.e.* no CDI (33)) in contrast to their properties in transfected HEK-293 cells (23).

Electrophysiological analysis of $Ca_v1.4$ is challenged by the small current densities produced by these channels in heterologous expression systems. One strategy to overcome this hurdle is to fuse a portion of $Ca_v1.4$ (*e.g.* the CTM) to the core of $Ca_v1.2$ or $Ca_v1.3$ channels, giving rise to more robust currents (23, 34). Another caveat is that virtually all studies to date have utilized auxiliary $Ca_v\beta$ and $\alpha_2\delta$ subunits that may not be associated with native $Ca_v1.4$ channel complexes in photoreceptors. Of the 4 $Ca_v\beta$ and $\alpha_2\delta$ variants that have been characterized (35, 36), β_2 and $\alpha_2\delta_4$ are required for vision in mice (37–39). We previously showed that most photoreceptor $Ca_v1.4$ channels contain an unusual β_2 splice variant ($\beta_{2\times13}$) as well as $\alpha_2\delta_4$ (40). To gain insights into how alternative splicing affects $Ca_v1.4$ channels containing $\beta_{2\times13}$ and $\alpha_2\delta_4$, we analyzed the electrophysiological properties of new $Ca_v1.4$ splice variants that we discovered while isolating cDNAs encoding $Ca_v1.4$ from human retina. Unlike $Ca_v1.4$ ex43*, which lacks the C-terminal 256 amino acids of the channel (23), these variants lack only exon 47, which deletes part of the CTM, but leaves the remaining C-terminal domain intact. We show that these variants are expressed at significant levels in human retina, and exhibit hyperpolarized voltages of activation and CDI similar to $Ca_v1.4$ ex43*. CaBP4 binds to and inhibits CDI of channels lacking exon 47, although it does not further enhance the hyperpolarized voltage-dependent activation of these channels. We conclude that exon 47 encodes critical determinants for regulating CDI and activation in a heterologous expression system, but that the presence of CaBP4 would likely nullify the CDI while not affecting the activation properties of these variants *in vivo*. Our results highlight the importance of analyzing Ca_v channels in the presence of known modulators for understanding the impact of alternative splicing on the properties of the native channels.

Results

Identification of Novel $Ca_v1.4$ Distal C-terminal Splice Variants in Human Retina—Using RT-PCR to generate a cDNA construct corresponding to human $Ca_v1.4$ from retinal RNA, we amplified a shorter product than expected with primers flanking nucleotides 3913 to 5934 of the cDNA encoding the full-length channel ($Ca_v1.4_{FL}$). Sequencing revealed that this fragment lacked the first 21 amino acids of exon 45 (p45) due to an alternative 3′ splice site in exon 45. This fragment was also missing exon 47 ($Ca_v1.4\Delta$ex p45,47; Figs. 1, *A–C*, and 2, *A* and *B*). Interestingly, $Ca_v1.4\Delta$ex p45,47 was detected in retinal samples from both human and monkey but not from mouse (Fig. 2*A*). The inability to measure $Ca_v1.4\Delta$ex p45,47 in mouse retina could be due to expression of $Ca_v1.4\Delta$ex p45,47 primarily in cone photoreceptors, which are more abundant in the retina of primates than mice. To test this, we compared the expression of $Ca_v1.4_{FL}$ and $Ca_v1.4\Delta$ex p45,47 in the cone-rich macula of monkey retina. No significant difference was observed between the ratio of $Ca_v1.4_{FL}$ and $Ca_v1.4\Delta$ex p45,47 in the macula compared with the peripheral retina of the monkey (Fig. 2, *C* and *D*). Therefore, $Ca_v1.4\Delta$ex p45,47 is unlikely to be more enriched in cones compared with rods. Quantitative PCR revealed that $Ca_v1.4\Delta$ex p45,47 was highly expressed in human and monkey retina, albeit at 20–150 lower levels than $Ca_v1.4_{FL}$ (Fig. 2, *B–D*; see Table 1 for primer sequences). In additional experiments, we detected $Ca_v1.4$ transcripts that had the single partial deletion of exon 45 ($Ca_v1.4\Delta$ex p45) or full deletion of exon 47 ($Ca_v1.4\Delta$ex47). Of these, $Ca_v1.4\Delta$ex p45 was the most abundant (Fig. 3, *A–C*).

$Ca_v1.4$ Variants Lacking Exon 47 Exhibit Robust CDI—Although C-terminal splice variants including $Ca_v1.4\Delta$ex p45 have been characterized (23), those lacking exon 47 have not. Because deletion of exon 47 removes part of the CTM (Fig. 1, *A* and *B*), we predicted that its deletion might affect CDI and voltage-dependent activation. We tested this in whole cell patch clamp recordings of HEK293T cells transfected with $Ca_v1.4_{FL}$, $Ca_v1.4\Delta$ex p45, $Ca_v1.4\Delta$ex47, or $Ca_v1.4\Delta$ex p45,47. Cells were cotransfected with cDNAs encoding the auxiliary $\beta_{2\times13}$ and $\alpha_2\delta_4$ subunits that co-assemble with $Ca_v1.4$ in the retina (40). To study CDI, we compared inactivation of Ca^{2+} currents (I_{Ca}) with that of Ba^{2+} currents (I_{Ba}). Inactivation was measured as the residual current amplitude at the end of the pulse normalized to the peak current amplitude (Fractional *I*); CDI was calculated as F_{CDI} (difference in Fractional I_{Ca} and mean Fractional I_{Ba} at −20 mV).

As shown previously, $Ca_v1.4_{FL}$ currents showed little inactivation during 1-s depolarizations regardless of whether Ca^{2+} or

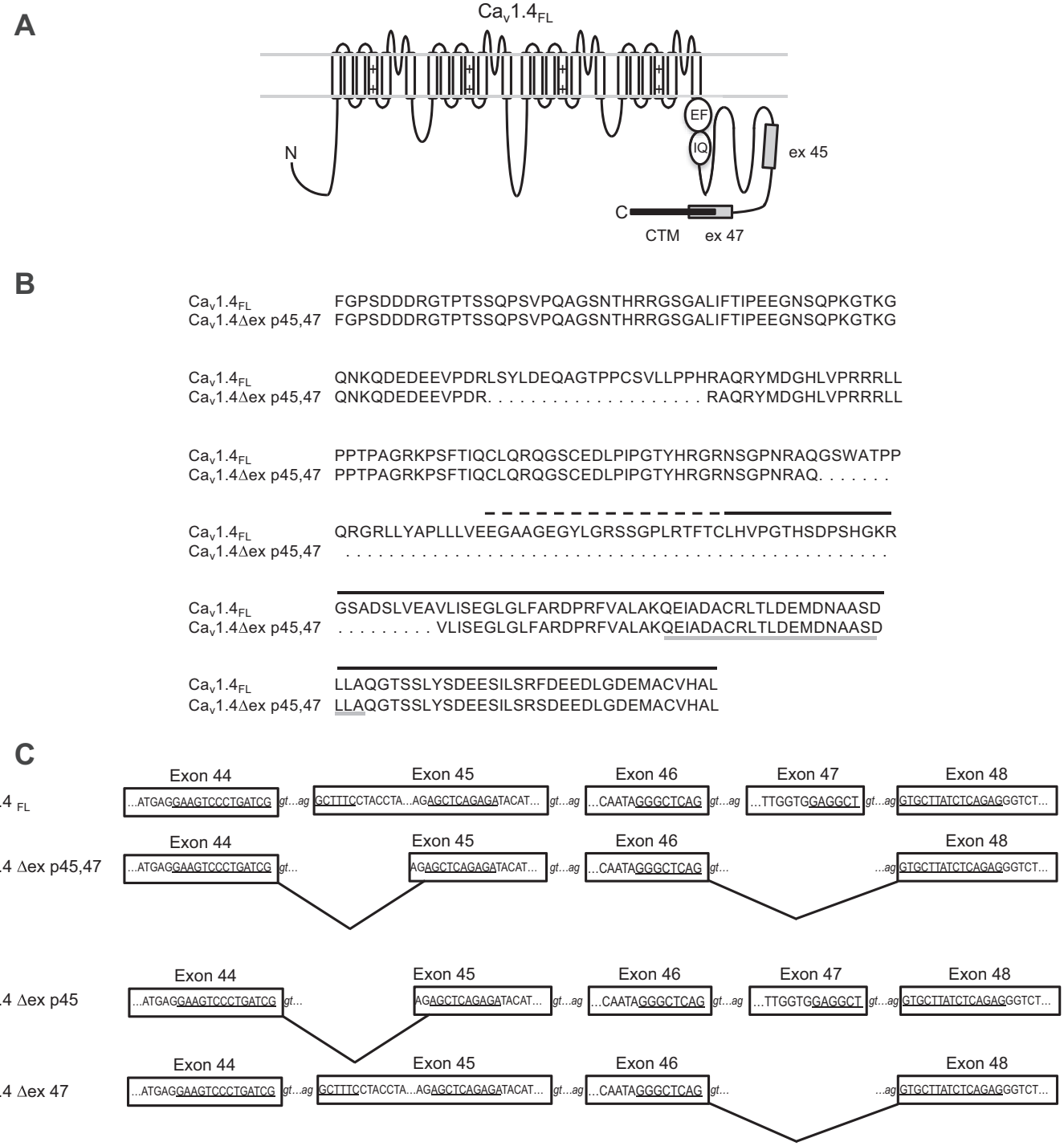

FIGURE 1. **Alternative $Ca_v1.4$ splice variants lacking portions of the C-terminal domain.** *A,* schematic of $Ca_v1.4_{FL}$ highlighting CDI-regulatory motifs (IQ, EF), CTM, and exons 45 and 47. *B,* alignment of the sequence in the C-terminal domain of human $Ca_v1.4$ from amino acids 1693 to 1977 and corresponding sequence in $Ca_v1.4\Delta$ex p45,47. The amino acids deleted in the variant are indicated by *dots*. *Black line*, CTM described by Wahl-Scott *et al.* (19). *Dashed line*, additional N-terminal sequence of the CTM described by Singh *et al.* (22). *Gray line*, previously reported determinants for CDI inhibition (19, 22). *C,* exon-intron junctions of exon 44 to exon 48 in $Ca_v1.4_{FL}$, $Ca_v1.4\Delta$ex p45, $Ca_v1.4\Delta$ex47, and $Ca_v1.4\Delta$ex p45,47.

Ba^{2+} was used as the permeant ion (Fig. 4*A*). The same was true for $Ca_v1.4\Delta$ex p45 (Fig. 4*B*). There was no significant difference in F_{CDI} for $Ca_v1.4_{FL}$ (0.05 ± 0.02, $n = 4$) and $Ca_v1.4\Delta$ex p45 (0.03 ± 0.02, $n = 8$; $p = 0.08$). In contrast, deletion of exon 47 caused robust inactivation of I_{Ca}, whereas I_{Ba} inactivation was unchanged (Fig. 4*C*). F_{CDI} was significantly greater (~12-fold) for $Ca_v1.4\Delta$ex47 (0.60 ± 0.02, $n = 13$; $p < 0.01$, by t test) compared with $Ca_v1.4_{FL}$. We next determined if exon 45 might act synergistically with exon 47 in regulating CDI. Although CDI was robust for $Ca_v1.4\Delta$ex p45,47 (0.65 ± 0.03, $n = 11$), it was not significantly different from that for $Ca_v1.4\Delta$ex47 ($p = 0.08$, by t test). These results indicate that exon 47 but not exon 45 contains critical determinants for suppressing CDI of $Ca_v1.4_{FL}$.

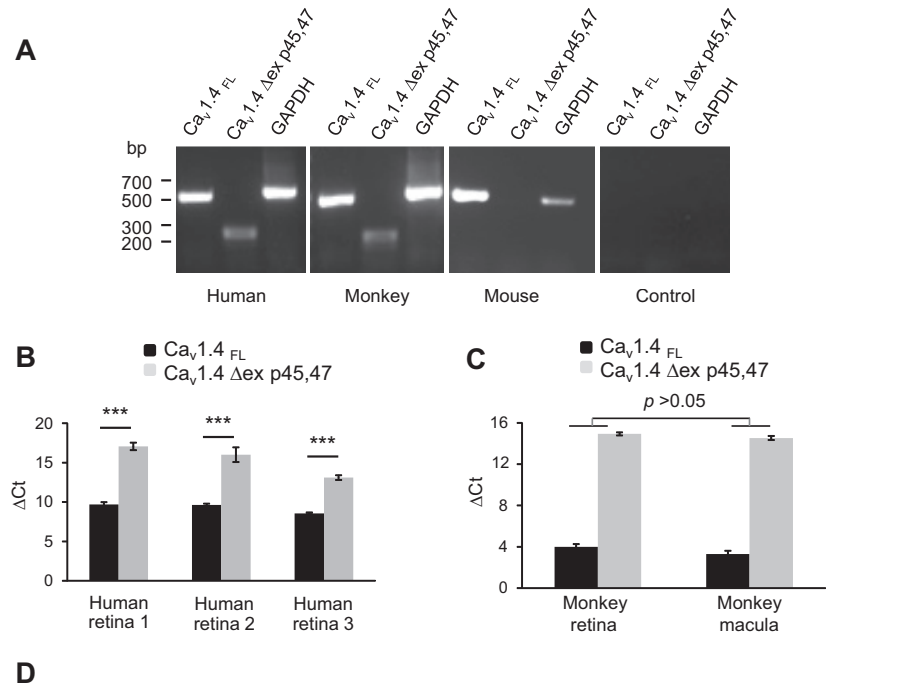

D

Species RNA	$Ca_v1.4_{FL}$ ΔCt (mean $Ca_v1.4_{FL}$ Ct – mean GAPDH Ct)	$Ca_v1.4$ Δ ex p45,47 ΔCt (mean $Ca_v1.4$ Δ ex p45,47 Ct – mean GAPDH Ct)	ΔΔCt (mean $Ca_v1.4_{FL}$ ΔCt – mean $Ca_v1.4$ Δ ex p45,47 ΔCt)	Normalized $Ca_v1.4_{FL}$ RNA relative to $Ca_v1.4$ Δ ex p45,47 RNA or $2^{-\Delta\Delta Ct}$
Human retina 1	9.69 ± 0.28	17.07 ± 0.48	-7.38 ± 0.48	166.7 ±55
Human retina 2	9.63 ± 0.17	16.01 ± 0.93	-6.38 ± 0.93	83.3 ± 53.9
Human retina 3	8.56 ± 0.12	13.11 ± 0.30	-4.55 ± 0.30	23.5 ± 4.9
Monkey retina	4.00 ± 0.27	14.93 ± 0.15	-10.93 ± 0.15	1953.2 ± 206.3
Monkey macula	3.30 ± 0.32	14.53 ± 0.20	-11.27 ± 0.20	2483.8 ± 350.3

FIGURE 2. **Expression of $Ca_v1.4_{FL}$ and $Ca_v1.4\Delta$ex p45,47 in the retina.** *A,* RT-PCR analysis of $Ca_v1.4$ and $Ca_v1.4\Delta$ex p45,47 expression in human, monkey, and mouse retina with primers as indicated in Table 1 (rows 1 to 6). *B,* qPCR analysis of $Ca_v1.4$ and $Ca_v1.4\Delta$ex p45,47 expression in human retina. Values represent mean ΔC_t values (C_t values for $Ca_v1.4$ and $Ca_v1.4\Delta$ex p45,47 normalized to the C_t values of the internal standard GAPDH) for all RNA preparations. (***, $p < 0.001$, unpaired *t* test, $n = 3$.) Primers are indicated in Table 1 (rows 1, 2). *C,* qPCR analysis of $Ca_v1.4_{FL}$ and $Ca_v1.4\Delta$ex p45,47 expression in monkey retina and fovea. Legend as described for *B*. Primers are indicated in Table 1 (rows 3, 4). *D,* fold-difference in transcript levels of $Ca_v1.4$ and $Ca_v1.4\Delta$ex p45,47 in human retina and in monkey retina and macula. qPCR data in *C* were analyzed using the $2^{-\Delta\Delta Ct}$ as described by Livak *et al.* (41). Fold-differences in C_t values between $Ca_v1.4$ and $Ca_v1.4\Delta$ex p45,47 were calculated after normalization to the GAPDH control. Data represent mean ± S.D. ($n = 3$).

$Ca_v1.4$ Variants Lacking Exon 47 Exhibit Activation at More Negative Voltages Than $Ca_v1.4_{FL}$—In plots of current density against voltage (I-V), only $Ca_v1.4$ channels lacking exon 47 exhibited an increase in current density, although both $Ca_v1.4\Delta$ex47 and $Ca_v1.4\Delta$ex p45,47 activated at more negative voltages than $Ca_v1.4_{FL}$ (Table 2; Fig. 5, *A–C*). To more rigorously characterize the voltage dependence of channel activation, we plotted the normalized tail current amplitudes against test voltage (Fig. 5, *D–F*). Boltzmann fits of the data indicated a significant effect of exon 47 deletion on the half-maximal voltage (V_h) and slope (k). The V_h was significantly more negative and k was steeper for $Ca_v1.4\Delta$ex47 and $Ca_v1.4\Delta$ex p45,47 than for $Ca_v1.4_{FL}$ (Fig. 5, *E* and *F*; Table 3). In contrast, there was no significant difference in these parameters for $Ca_v1.4\Delta$ex p45 and $Ca_v1.4_{FL}$ (Fig. 5*D*; Table 3). These results indicate that exon 47 encodes molecular determinants within the CTM that regulate voltage-dependent activation of $Ca_v1.4_{FL}$.

Deletion of Exon 47 Does Not Affect Binding of $Ca_v1.4$ to CaBP4, but Prevents Effects of CaBP4 on Activation—CaBP4 is a CaM-like modulator of $Ca_v1.4$ in photoreceptors, and binds to the same site(s) as CaM in the C-terminal domain (CT) of $Ca_v1.4$ (31, 32). To test if splicing of exons 45 and 47 affected the interaction of CaBP4 with the channel, we used FLAG antibodies to immunoprecipitate FLAG-tagged $Ca_v1.4$ variants in HEK-293 cells transfected alone or cotransfected with CaBP4. Western blotting analysis with anti-CaBP4 antibodies revealed the co-immunoprecipitation of CaBP4 with both FLAG-$Ca_v1.4_{FL}$ and FLAG-$Ca_v1.4\Delta$ex p45,47 (Fig. 6*A*). As we have found previously for FLAG-tagged $Ca_v1.3$ (42), channel protein was detected by Western blotting only after immunoprecipitation and not in the cell lysates presumably due to limited sensitivity of the FLAG antibodies. These co-immunoprecipitated proteins were not detected when control mouse IgG was used instead of anti-FLAG antibodies. Although these results suggested that CaBP4 binds equally well to both $Ca_v1.4$ and $Ca_v1.4\Delta$ex p45,47, it was possible that our co-immunoprecipitation assay did not report subtle changes in CaBP4 binding affinity. Therefore, we compared CaBP4 binding to these variants in an ELISA binding assay. For these experiments, we generated SUMO-tagged fusion proteins corresponding to the CT of $Ca_v1.4_{FL}$ and $Ca_v1.4\Delta$ex p45,47 and compared their binding to 96-well plates coated with GST-tagged CaBP4. Binding of $Ca_v1.4\Delta$ex p45,47 CT to CaBP4 was similar to that by $Ca_v1.4_{FL}$ CT (Fig. 6*B*). Signals representing CaBP4 binding were specific

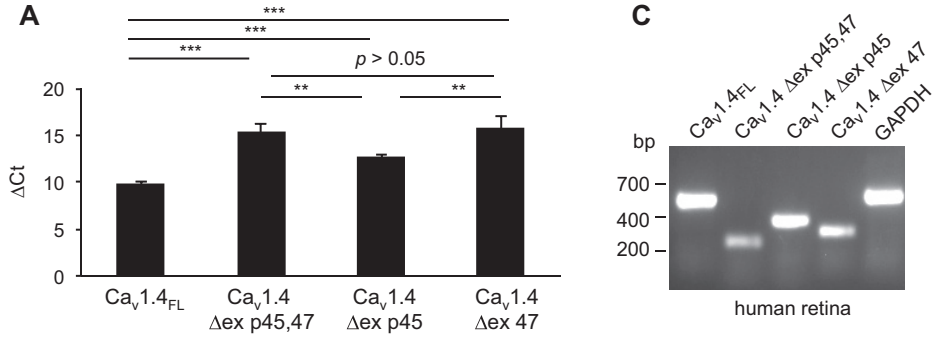

B

$Ca_v1.4$ variant	ΔCt (mean $Ca_v1.4$ variant – mean GAPDH Ct)	ΔΔCt (mean $Ca_v1.4_{FL}$ ΔCt – mean $Ca_v1.4$ variant ΔCt)	Normalized $Ca_v1.4_{FL}$ RNA relative to $Ca_v1.4$ variants RNA or $2^{-\Delta\Delta Ct}$
$Ca_v1.4_{FL}$	9.77 ± 0.33		
$Ca_v1.4$ Δex p45,47	15.33 ± 0.94	-5.56 ± 0.94	47 ± 30.7
$Ca_v1.4$ Δex p45	12.63 ± 0.34	-2.85 ± 0.34	7.25 ± 1.7
$Ca_v1.4$ Δex 47	15.72 ± 1.25	-5.95 ± 1.25	61.8 ± 53

FIGURE 3. **Comparison of expression of $Ca_v1.4_{FL}$ with C-terminal splice variants in the human retina.** *A,* qPCR analysis of the expression of $Ca_v1.4_{FL}$ and exon 45/47 variants in human retina. Legend as described in Fig. 2*B*, primers as indicated in Table 1 (rows 2, 7, to 9). *B,* fold-difference in transcript levels between $Ca_v1.4_{FL}$ and exon 45/47 variants in human retina. Legend as described in Fig. 2*D*. (**, $p \leq 0.008$; ***, $p < 0.001$; by unpaired *t* test, $n = 3$.) No significant difference between transcript levels of $Ca_v1.4$Δex p45,47 and $Ca_v1.4$Δex 47. *C,* RT-PCR analysis of $Ca_v1.4$ and exon 45/47 variants in human retina.

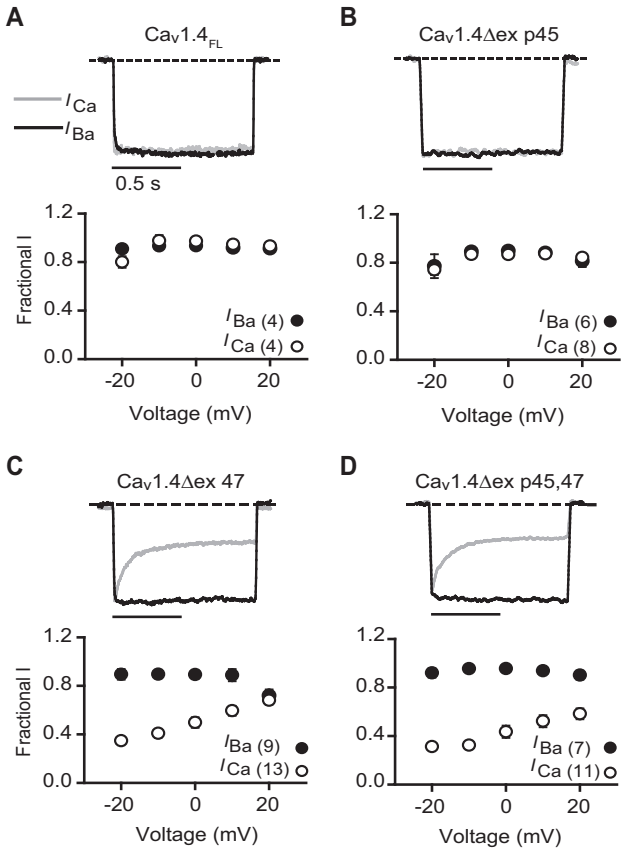

FIGURE 4. **$Ca_v1.4$ variants lacking exon 47 exhibit CDI.** *Top*, representative current traces for I_{Ba} (*black*) and I_{Ca} (*gray*) for $Ca_v1.4_{FL}$ (*A*), $Ca_v1.4$Δex p45 (*B*), $Ca_v1.4$Δex47 (*C*), and $Ca_v1.4$Δex p45,47 (*D*). Currents were evoked by 1-s pulses from −80 to +20 mV. *Bottom*, I_{Ca} or I_{Ba} were evoked by 1-s pulses from −80 mV to various test voltages. Inactivation was measured as the current amplitude at the end of the pulse normalized to the peak current (Fractional I) and plotted against test voltage. *Parentheses* indicate the number of cells.

TABLE 2
Parameters for Boltzmann fits of I-V relationships

Construct	V_h	*k*	*n*
$Ca_v1.4_{FL}$	7 ± 1.0	−9 ± 0.4	6
$Ca_v1.4$Δex p45	4 ± 1.0	−10 ± 0.3	7
$Ca_v1.4$Δex 47	−1 ± 1.0[a]	−10 ± 0.3	11
$Ca_v1.4$Δex p45,47	0.03 ± 1.0[a]	−10 ± 0.3	7

[a] $p < 0.001$; compared with $Ca_v1.4_{FL}$ (one-way ANOVA followed by Bonferroni post test).

in that no binding was detected on plates coated with GST alone (not shown) or with $Ca_v1.4$ CT lacking the CaM-binding region in the proximal CT ($Ca_v1.4$ΔpCT Fig. 6*B*). We also tested how deletion of exons 45 and 47 affect CaM binding to the CT. Consistent with previous *in vitro* analyses of CaM binding to the $Ca_v1.4_{FL}$ CT (19), purified CaM bound to the $Ca_v1.4_{FL}$ CT. CaM bound similarly to the CT of $Ca_v1.4$Δex p45,47, but binding was abolished by deletion of the CaM/CaBP4 binding site (Fig. 6*C*). Taken together, our results show that deletion of exon 47 and part of exon 45 does not affect binding of CaM or CaBP4 to $Ca_v1.4$.

We next determined if deletion of exon 47 affected modulation by CaBP4. For these experiments, we used $Ca_v1.4$Δex 47 because the splicing of exon 45 had no effect on the electrophysiological properties of the channel (Figs. 4 and 5). Although CaBP4 causes a negative shift in voltage-dependent activation of $Ca_v1.4_{FL}$ (31, 32), it did not similarly affect $Ca_v1.4$Δ ex47. There was no significant difference in I-V or normalized tail current-voltage relationships in cells expressing $Ca_v1.4$Δex 47 alone and those co-expressing CaBP4 (Fig. 7, *A* and *B*; Table 4). However, CaBP4 did blunt the strong inactivation of $Ca_v1.4$Δ ex47 I_{Ca}. CaBP4 caused a significant 2-fold reduction in the amount of I_{Ca} inactivation of $Ca_v1.4$Δ ex47 (Fractional I_{Ca} = 0.30 ± 0.1, $n = 5$ for $Ca_v1.4$Δ ex47 alone *versus* 0.56 ± 0.10, n = 7 for $Ca_v1.4$Δ ex47 + CaBP4; $p < 0.02$ by *t* test; Fig. 7*C*). We

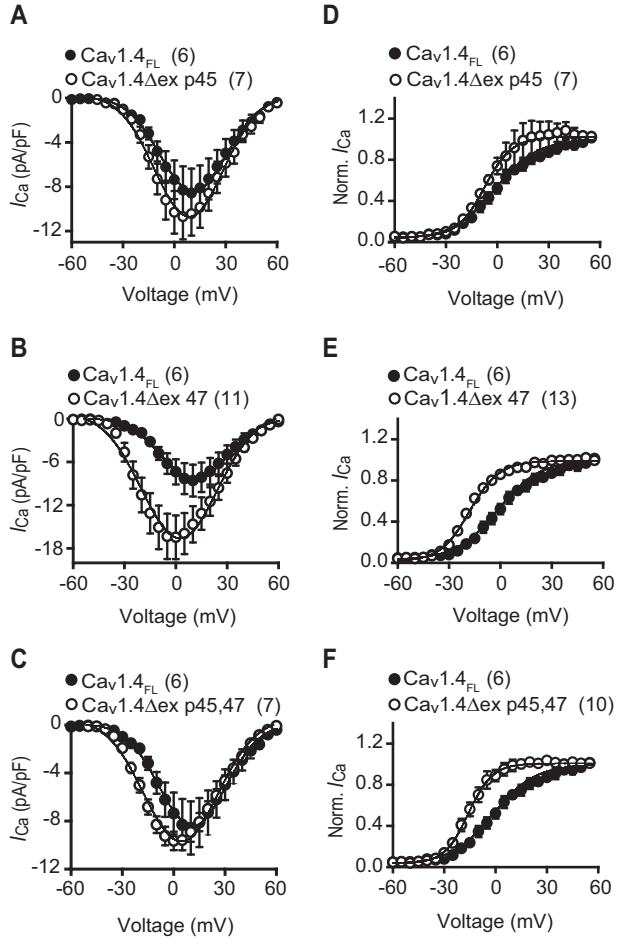

FIGURE 5. **Splicing of exon 47 but not exon 45 significantly affects voltage-dependent activation of $Ca_v1.4$.** *A–C*, normalized current-voltage (*I–V*) plots for I_{Ca}. Currents were evoked by 50-ms pulses from −80 mV to various test voltages. *D–F*, normalized tail current − voltage plots for $Ca_v1.4_{FL}$ and $Ca_v1.4$ splice variants. Tail currents were evoked by 10-ms pulses from −80 mV to various test voltages with 2-ms repolarization to −60 mV during which the peak tail current amplitude was measured. Current amplitudes were normalized to that evoked by a +60-mV pulse and plotted against the test voltage. *Parentheses* indicate the number of cells.

TABLE 3

Parameters for Boltzmann fits of normalized tail-current voltage curves

Construct	V_h	k	n
$Ca_v1.4_{FL}$	−4 ± 1.8	−10 ± 0.3	6
$Ca_v1.4$Δex p45	−7 ± 1.7	−8 ± 1.0	7
$Ca_v1.4$Δex 47	−18 ± 1.0[a]	−6 ± 1.2[b]	13
$Ca_v1.4$Δex p45,47	−15 ± 2.0[a]	−7 ± 1.0[b]	10

[a] $p < 0.001$ compared with $Ca_v1.4_{FL}$ (one-way ANOVA followed by Bonferroni post-test).
[b] $p < 0.05$ compared with $Ca_v1.4_{FL}$ (one-way ANOVA followed by Bonferroni post test).

conclude that exon 47 is dispensable for the ability of CaBP4 to antagonize effects of CaM on CDI of $Ca_v1.4_{FL}$, but is required for CaBP4 modulation of voltage-dependent activation.

Discussion

Our study reveals new insights into how splice variation of the C-terminal domain affects the properties of $Ca_v1.4$ channels in the retina. First, we report that novel $Ca_v1.4$ splice variants that lack exon 47 alone ($Ca_v1.4$Δex 47) and/or partial deletion of exon 45 ($Ca_v1.4$Δex p45,47) are highly expressed in primate but not mouse retina. Second, exon 47 contains crucial determinants within the CTM for suppressing CDI and voltage-dependent activation. Finally, exon 47 is also needed for the functional modulation of channel activation by CaBP4, but not for the physical interaction of CaBP4 with the $Ca_v1.4$ C-terminal domain. These findings underscore the importance of the distal C-terminal domain in controlling the intrinsic biophysical properties of $Ca_v1.4$ as well as its modulation by CaM and CaBP4.

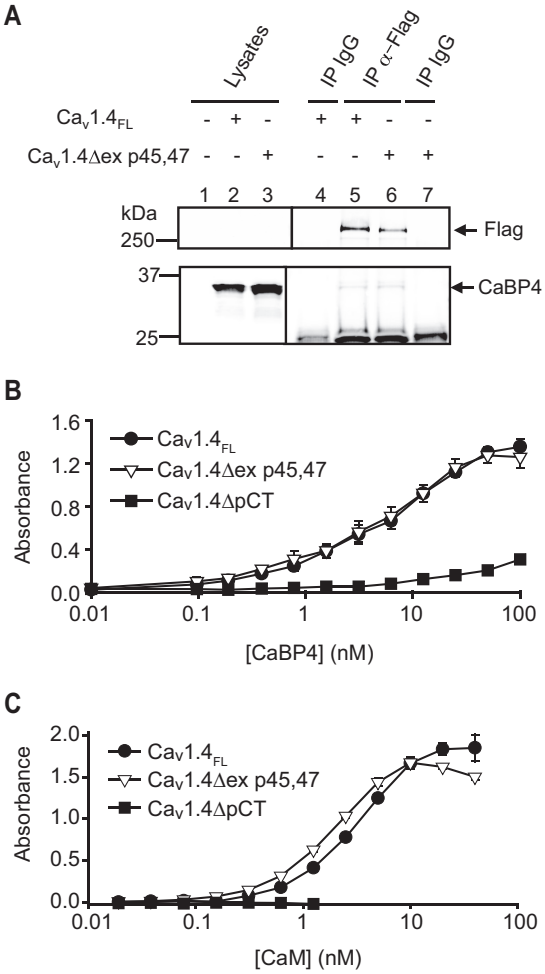

FIGURE 6. **CaBP4 interacts with $Ca_v1.4_{FL}$ and $Ca_v1.4$Δex p45,47.** *A*, HEK-293 cells were co-transfected with CaBP4 and FLAG-tagged $Ca_v1.4$ (*lanes 2*, *4*, and *5*) or $Ca_v1.4$Δex p45,47 (*lanes 3*, *6*, and *7*). Cell lysates were subject to immunoprecipitation (*IP*) with FLAG antibodies (*lanes 5* and *6*) or control IgG (*lanes 4* and *7*). Blots were probed with antibodies against FLAG (*top*) or CaBP4 (*bottom*). *Lanes 1–3* represent lysates from untransfected (*lane 1*) or transfected (*lanes 2* and *3*) cells. *B*, SUMO-tagged CT from $Ca_v1.4_{FL}$, $Ca_v1.4$Δex p45,47, or $Ca_v1.4_{FL}$ lacking the CaM/CaBP4 binding site in proximal CT ($Ca_v1.4$ΔpCT) was incubated with GST or GST-CaBP4-coated wells for ELISA. Binding was detected with anti-SUMO antibodies. Points represent mean ± S.D. after subtraction of signals corresponding to nonspecific binding to GST ($n = 3$). *C*, same as in *B* but incubation with GST-CaM-coated wells for ELISA.

Exon 47 as a Modulator of $Ca_v1.4$ CDI and Voltage-dependent Activation—The distal CT domain has emerged as a key regulator of CDI of $Ca_v1.3$ and $Ca_v1.4$ (19, 22, 43). Alternative splice variants of $Ca_v1.3$ and $Ca_v1.4$ lacking this domain exhibit stronger CDI than the corresponding full-length channels (23, 43, 44). For both $Ca_v1.3$ and $Ca_v1.4$, CDI suppression is mediated by a CTM corresponding to the final ~100–150 amino

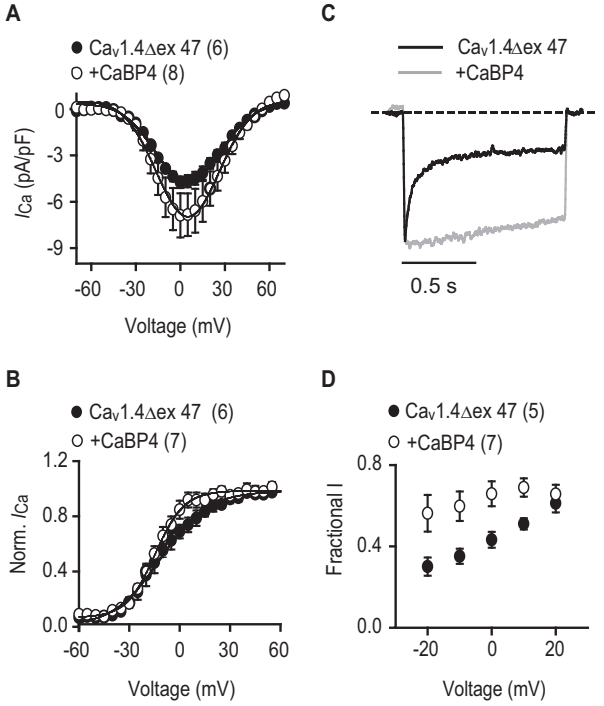

FIGURE 7. **CaBP4 modulates CDI but not voltage-dependent activation of $Ca_v1.4\Delta$ ex47.** *A* and *B*, normalized I-V (*A*) and tail current-voltage plots (*B*) for I_{Ca} in cells transfected with $Ca_v1.4\Delta$ex 47 alone or with CaBP4. Data were obtained as described in Fig. 5, *A–F*. *C*, representative traces for I_{Ca} evoked by a 1-s test pulse from −80 to 0 mV in cells transfected as in *A* and *B*. *D*, fractional I was obtained as in Fig. 4 and plotted against test voltage. *Parentheses* indicate the number of cells.

TABLE 4

Parameters for Boltzmann fits of I-V and normalized tail-current voltage curves

Construct	V_h	K	n
I-Vs			
$Ca_v1.4\Delta$ex 47 alone	2 ± 2.0	−11 ± 0.5	6
$Ca_v1.4\Delta$ex 47+CaBP4	−0.2 ± 1.6	−10 ± 0.3[a]	8
Normalized tail-voltage			
$Ca_v1.4\Delta$ex 47 alone	−13 ± 3.0	−10 ± 1.0	6
$Ca_v1.4\Delta$ex 47+CaBP4	−14 ± 1.3	−8 ± 1.0	7

[a] $p < 0.001$ compared with $Ca_v1.4\Delta$ex47 (control) (Student's *t* test).

acids (aa) of the channel protein (19, 22, 43). The underlying mechanism is controversial and involves binding of the CTM to a site in the proximal CT, which may physically displace CaM from the channel (22, 43). Alternatively, the CTM binding to the proximal CT is not competitive, but allosterically alters the binding of CaM in a way that weakens CDI (20). This interaction of the CTM with the proximal CT could be affected by sequences between the two domains, including exon 45 (Fig. 1). However, we did not find that splicing out part of exon 45 affected CDI or voltage-dependent activation (Figs. 4 and 5). These results are consistent with previous analyses of the partial deletion of exon 45 in chimeric $Ca_v1.2$-$Ca_v1.4$ (23), and with the inconsequential effects of alternative splicing of the analogous exon 44 of $Ca_v1.3$ (43).

By contrast, deletion of exon 47 had dramatic effects on CDI. For $Ca_v1.4\Delta$ex 47 and $Ca_v1.4\Delta$ex p45,47 variants (Fig. 4), CDI was as robust as that caused by removal of the entire CTM (19, 20, 22). At first glance, this result may seem at odds with previous findings that truncation of the final 55 aa distal to exon 47 disabled the ability of the CTM to suppress CDI (22). Because deletion of the last 32 amino acids was ineffective in this regard, it was concluded that the stretch of 20 aa between aa −55 and −32 from the C terminus contains the molecular determinants for CDI suppression (19, 22). Our results show that these 20 aa are not sufficient to support the function of the CTM because their presence in $Ca_v1.4\Delta$ex47 and $Ca_v1.4\Delta$ex p45,47 was not able to suppress CDI (Fig. 4, *C* and *D*). The region encoded by exon 47 may enable proper folding of the CTM and/or provide key contact points required for the intramolecular interaction with the proximal CT. Consistent with both possibilities, deletion of portions of exon 47 prevented binding of the CTM to the proximal CT (20).

In addition to suppressing CDI, the CTM inhibits voltage-dependent activation of Ca_v1 channels. For $Ca_v1.2$, the distal CT is proteolytically cleaved but remains noncovalently attached to the proximal CT, causing a positive shift in V_h (45). Although there is no evidence that the distal CT is cleaved *in vivo* for $Ca_v1.3$ (46) or $Ca_v1.4$, the distal CT of these channels autoinhibits voltage-dependent activation. $Ca_v1.3$ or $Ca_v1.4$ mutants or splice variants lacking the CTM exhibit negative shifts in V_h compared with full-length channels (19, 20, 22, 23, 43, 44). Our findings indicate that exon 47 is a key element within the CTM that regulates activation because V_h for $Ca_v1.4$ variants lacking exon 47 were ~15 mV more negative than that of $Ca_v1.4_{FL}$ (Fig. 5, Table 3). How the CTM regulates voltage-dependent activation of $Ca_v1.4$ is not entirely clear but could involve inhibition of movement of the voltage-sensing domains. However, for $Ca_v1.2$ and $Ca_v1.3$, the positive shift in V_h due to autoinhibition by the CTM is attributed to weaker coupling of voltage sensor movement to opening of the channel pore (45, 47). Addressing the underlying mechanism for $Ca_v1.4$ would require analysis of the voltage dependence of gating charges representing movement of the voltage sensors (48). These experiments would be technically quite challenging for $Ca_v1.4$ channels, which produce very modest current density in heterologous expression systems compared with $Ca_v1.2$ and $Ca_v1.3$ (40).

Exon 47 and CaBP4 Modulation of $Ca_v1.4$—CaBP4 and other CaBP family members are potent suppressors of CDI of $Ca_v1.2$ and $Ca_v1.3$ channels (reviewed in Ref. 49). Compared with the analogous CTM regions of $Ca_v1.2$ and $Ca_v1.3$, the CTM of $Ca_v1.4_{FL}$ more completely abolishes CDI such that an effect of CaBP4 on suppressing CDI can only be observed in $Ca_v1.4_{FL}$ channels lacking the CTM (32). Nevertheless, CaBP4 does bind to $Ca_v1.4_{FL}$ and enhances activation through a −10 mV shift in V_h (31, 32). The inability of CaBP4 to similarly promote voltage-dependent activation of channels lacking exon 47 (Fig. 7, *A* and *B*) indicates a key role for this exon in supporting CaBP4 modulation. CaBP4 still binds to the CT (Fig. 6*B*) and markedly suppresses CDI of channels lacking exon 47 (Fig. 7, *C* and *D*), which argues against the possibility that deletion of exon 47 prevents the physical interaction of CaBP4 with the channel. Our results agree with previous findings that deletion of the entire previously defined CTM does not abrogate the physical interaction of CaBP4 with $Ca_v1.4_{FL}$, despite preventing effects of CaBP4 on voltage-dependent activation (32). As discussed for its role in regulating CDI, exon 47 may contribute to the structure and/or function of the CTM, which is necessary for

transducing the effect of CaBP4 binding on activation. Alternatively, the negative shift in activation of $Ca_v1.4\Delta$ex p45,47 compared with $Ca_v1.4_{FL}$ may biophysically occlude further modulation by CaBP4.

Physiological Relevance of C-terminal Splicing of Exons 45 and 47 in the Retina—Our electrophysiological recordings utilized channels containing $\beta_{2\times13}$ and $\alpha_2\delta_4$ because these subunits co-assemble with $Ca_v1.4$ in photoreceptor terminals (40). Although other β and $\alpha_2\delta$ subunits may be expressed in the retina (50), strong CDI and enhanced voltage-dependent activation are seen upon removal of the CTM from $Ca_v1.4$ channels coexpressed with β_3 and $\alpha_2\delta_1$ subunits (22). Therefore, these properties in $Ca_v1.4\Delta$ex 47 and $Ca_v1.4\Delta$ex p45,47 are not likely to be significantly affected by differences in auxiliary subunit composition.

To compensate for the relatively small currents carried by $Ca_v1.4$ compared with other Ca_v channels, we used a high concentration (20 mM) of Ca^{2+} or Ba^{2+} in the extracellular recording solution. Due to charge screening effects (51, 52), this would cause channels to activate at more depolarized voltages than in physiological solutions. Based on activation properties of $Ca_v1.4$ in 2 mM extracellular Ca^{2+} (13), the V_h values reported here (Tables 2–4) should be ~20 mV more positive than would be expected for $Ca_v1.4$ channels *in vivo*. Taking this into account, the channels lacking exon 47 would be expected to support ~3-fold higher levels of Ca^{2+} influx compared with $Ca_v1.4_{FL}$ at the photoreceptor membrane potential in darkness (−30 to −40 mV (14, 15)). However, this difference may be offset by the presence of CaBP4 in photoreceptor terminals. As a consequence of modulation by CaBP4 (31, 32), $Ca_v1.4_{FL}$ should exhibit hyperpolarized voltage dependence of activation similar to that of $Ca_v1.4\Delta$ex 47 and $Ca_v1.4\Delta$ex p45,47 (Fig. 5, *E* and *F*). The negative activation properties of $Ca_v1.4_{FL}$ modulated by CaBP4, and exon 47-lacking $Ca_v1.4$ variants would promote presynaptic Ca^{2+} influx to support glutamate release at the photoreceptor membrane potential in darkness. This in turn would ensure mGluR6-mediated closure of nearly all postsynaptic TRPM1 channels, which at the rod-rod bipolar cell synapse, is necessary for the optimal encoding of dim light signals (53, 54). At the same time, CaBP4 would suppress CDI of $Ca_v1.4\Delta$ex 47 and $Ca_v1.4\Delta$ex p45,47, much like the CTM does for $Ca_v1.4_{FL}$ (Fig. 4). Thus, both exon 47-lacking channels and $Ca_v1.4_{FL}$ could mediate sustained Ca^{2+} influx necessary for tonic glutamate release in darkness, although via different mechanisms.

We do not discount the possibility that splicing of exons 45 and 47 could have effects in photoreceptors that are independent of the electrophysiological findings in our study. Like other ion channels, Ca_v channels interact with a variety of modulatory and scaffolding proteins that collectively regulate the cellular roles of these channels in different tissues (55). Because the CT of Ca_v1 channels is a major hotspot for such protein interactions, deletion of exon 47 and/or partial deletion of exon 45 could disrupt the association of the channel with a regulatory protein present in photoreceptor terminals that is not endogenously expressed in our heterologous expression system (*i.e.* HEK293T cells). As for other Ca_v splice variants (56), alternative splicing of exons 45 and 47 could be developmentally regulated and confer $Ca_v1.4$ channels with the ability to adjust their functional interactions according to maturational stage of the photoreceptor. Taken together, our results pinpoint exon 47 as a key determinant in the regulation of $Ca_v1.4$ activation and CDI by the CTM, and highlight the complexity of understanding the impact of alternative splicing for Ca_v channel function *in vivo*.

Experimental Procedures

Plasmids and Cloning of Human $Ca_v1.4$ Variants—The cloning of the human full-length $Ca_v1.4$ α_1 subunit ($Ca_v1.4_{FL}$) with an N-terminal FLAG epitope (GenBank™ number AF201304) in pcDNA3.1 vector, $\beta_{2\times13}$ (GenBank™ number AF465485), $\alpha_2\delta_4$ (GenBank™ number NM_172364), and CaBP4 (GenBank™ number AY 039217.1) was described previously (31, 40). For the cloning of $Ca_v1.4$ deleted from part of exon 45 (ex p45) and full exon 47 (ex 47; $Ca_v1.4\Delta$ex p45,47), a similar strategy to that used for the $Ca_v1.4_{FL}$ was followed (40). An F5 fragment (HindIII-TGA stop codon, covering nucleotides 3913 to 5934 in $Ca_v1.4_{FL}$) harboring these deletions was cloned into pcDNA3.1 containing F1 to F4 of $Ca_v1.4_{FL}$. To clone $Ca_v1.4\Delta$ex p45, the HindIII-NotI insert of pcDNA-$Ca_v1.4_{FL}$ covering fragment F5 was replaced with a fragment HindIII-SacI covering exon 33 to exon 45 from pcDNA-$Ca_v1.4\Delta$ex p45,47, the SacI restriction site being located just after the deletion, with a fragment SacI-NotI (exon 45 to exon 48) from pcDNA-$Ca_v1.4_{FL}$. To clone $Ca_v1.4\Delta$ex 47, the HindIII-NotI insert of pcDNA-$Ca_v1.4_{FL}$ covering fragment F5 was replaced with a fragment HindIII-SacI covering exon 33 to exon 45 from pcDNA-$Ca_v1.4_{FL}$ with a fragment SacI-NotI (exon 45 to exon 48) from pcDNA-$Ca_v1.4\Delta$ex p45,47.

To subclone the CT domain of $Ca_v1.4_{FL}$ and $Ca_v1.4\Delta$ex p45,47, a fragment encoding amino acids 1441 to the terminal stop codon was amplified by PCR with Pfx polymerase (Life Technologies). To remove the CaM binding site(s), a fragment encoding amino acids 1603 to the stop codon was also amplified. These PCR products were cloned into the pET-SUMO vector (Life Technologies) for fusion to both a His_6 and a SUMO tag. The fusion proteins were expressed in BL21(DE3)pLysS *Escherichia coli* after induction with 0.5 mM isopropyl 1-thio-β-D-galactopyranoside and purified on nickel-nitrilotriacetic acid columns according to the manufacturer's protocol.

CaBP4 was amplified by PCR from a human retina cDNA library and cloned into pentr-D-TOPO vector (Life Technologies). After sequencing, the cDNA was transferred by recombination into the pDest15 vector using the Gateway Technology System (Life Technologies) for fusion to a GST tag and expression in bacteria. The GST fusion proteins were expressed in BL21(DE3) pLysS *E. coli* after induction with 0.5 mM isopropyl 1-thio-β-D-galactopyranoside and purified on a glutathione column according to the manufacturer's protocol.

Quantitative PCR Analysis of Human and Monkey $Ca_v1.4$ and Their Splice Variants—All procedures were approved by the Institutional Animal Care and Use Committee of the University of Washington. Retinas from *Macaca nemestrina* were obtained at the University of Washington Regional Primate Center (Seattle, WA). Human retinas were obtained from

donors without known eye disease from the Lions Eye Bank of Oregon 4–10 h after death. Total RNA was isolated from the retina of human, monkey, or mouse using a RNeasy kit (Qiagen). The relative expression of splice variants was determined by a two-step quantitative PCR. Total RNA (1 μg) was subjected to first strand cDNA synthesis using SuperScript III reverse transcriptase and oligo(dT) in a volume of 20 μl according to the manufacturer's protocol (Life Technologies). For the qPCR analysis of the $Ca_v1.4\Delta$ex p45,47, primers were designed on the exon 44-alternate exon 45 joint (forward) and ~200 bp downstream on the exon 46-exon 48 joint (reverse, Table 1, row 2). For the $Ca_v1.4_{FL}$, primers were designed on the exon 44-exon 45 junction (forward) and ~460 bp downstream on the exon 47-exon 48 junction (reverse, Table 1, row 1). For the RT-PCR analysis of $Ca_v1.4\Delta$ex p45,47 in mouse, human, and monkey, similar primers were used as indicated in Table 1 (rows 1 to 6).

For comparison by qPCR of all the C-terminal variants with $Ca_v1.4_{FL}$, primers were designed to exon 45, exon 47, exon 44-alternate exon 45 joint, or exon 46-exon 48 joint (Table 1, rows 2 and 7–9). For normalization, primers were used to amplify glyceraldehyde-3-phosphate dehydrogenase (GAPDH, Table 1, rows 10 to 12). Reactions were carried out in triplicate using 0.5 μl of cDNA, 400 nM of each primer, and 10 μl of QuantiTect SYBR Green PCR mix (Qiagen) in a 20-μl total reaction volume. After an initial incubation at 95 °C for 15 min, the qPCR was carried out for 40 cycles of denaturation at 95 °C for 15 s, annealing at 68 °C for 30 s, and extension at 72 °C for 1 min on a ABI PRISM 7000 (Applied Biosystems). Single bands of the predicted size were verified by agarose gel electrophoresis. Threshold cycle was determined using the ABI Prism 7000 software. Data were analyzed by comparing cycle threshold (C_t) normalized to the C_t values of the internal control, GAPDH (ΔC_t value = C_t value of WT or variant − C_t value of GAPDH); standard deviation of $\Delta C_t = \sqrt{(\text{S.D. of variant or WT})^2 + (\text{S.D. of GAPDH})^2}$. The normalized C_t values of the $Ca_v1.4$ variants and $Ca_v1.4_{FL}$ were compared by determining $\Delta\Delta C_t$ = ΔC_t $Ca_v1.4_{FL}$ − ΔC_t $Ca_v1.4$ variant. Fold-induction was calculated as $2^{(-\Delta\Delta Ct)}$ (41).

Co-immunoprecipitation of $Ca_v1.4$ and CaBP4—HEK-293 cells were transfected with cDNAs encoding $Ca_v1.4_{FL}$ or $Ca_v1.4\Delta$ex p45,47, $\beta_{2\times13}$, $\alpha_2\delta_4$, and CaBP4. Three days later, whole cell lysates were prepared by incubation of transfected cells at 4 °C for 1 h in 20 mM Tris, pH 7.5, 150 mM NaCl, 1% Nonidet P-40, 0.5% sodium deoxycholate, 0.1 mM $MgCl_2$, 0.1 mM $CaCl_2$ and inhibitors of proteases (Sigma). Lysates were subject to centrifugation at 22,000 × *g* for 30 min and incubated with mouse IgG (purified on protein G plus agarose from mouse serum) or anti-FLAG antibodies (Sigma). After 1 h incubation at 4 °C, protein G-magnetic beads (Life Technologies) were added and the incubation proceeded for 3 h at 4 °C. After 4 washes with lysis buffer, proteins were eluted with SDS-sample buffer and analyzed by Western blotting with specific antibodies.

Enzyme-linked Immunoadsorbent Assay (ELISA)—Purified GST, GST-CaBP4, or GST-CaM fusion proteins (2 μg/ml in 100 mM sodium bicarbonate, pH 9.0) were bound to 96-well ELISA plates (200 ng/well) overnight at 4 °C. The wells were blocked with animal-free blocker (Vector laboratories) for 1 h at room temperature. 2-Fold dilutions of SUMO-$Ca_v1.4$ C-terminal domain (CT) fusion proteins in TBST_MC (50 mM Tris pH 7.5, 150 mM NaCl, 1 mM $MgCl_2$, 1 mM $CaCl_2$, 0.05% Tween 20) were added and reactions were incubated for 1 h at room temperature. After 3 washes in TBST-MC, bound $Ca_v1.4$ CT was detected with rat anti-SUMO antibodies (raised in rats and purified with SUMO proteins using a previously described method (40)) for 1 h at room temperature, followed by incubation with alkaline phosphatase-conjugated anti-rat antibodies. Reactions were incubated with *p*-nitrophenyl phosphate substrate (diluted in 100 mM Tris, pH 9.0, 50 mM $MgCl_2$, 100 mM NaCl) for 30 min at room temperature and the absorbance was measured at 405 nm with a microplate reader (Bio-Rad). The absorbance data of nonspecific binding of $Ca_v1.4$ to GST (negative control for binding to GST) was subtracted from that for binding of SUMO-$Ca_v1.4$ CT to GST-CaBP4.

Electrophysiology—HEK-293T cells were cultured in Dulbecco's modified Eagle's medium (Life Technologies) with 10% fetal bovine serum (Atlantic Biologicals) at 37 °C in 5% CO_2, and grown to 70–80% confluence. Cells plated in 35-mm dishes were co-transfected with cDNAs encoding human $Ca_v1.4$ α_1 (1.8 μg; $Ca_v1.4_{FL}$, $Ca_v1.4\Delta$ex p45, $Ca_v1.4\Delta$ex p45,47, or $Ca_v1.4\Delta$ex 47), $\beta_{2\times13}$ (0.6 μg), $\alpha_2\delta_4$ (0.6 μg), and enhanced green fluorescent protein (0.1 μg). FuGENE 6 transfection reagent (Promega) was used according to the manufacturer's protocol. Cells treated with the transfection mixture were incubated at 37 °C for 24 h prior to dissociation and maintenance at 30 °C prior to recording.

We have found that overexpression of CaBP4 has inhibitory effects on Ca_v channel current density, perhaps through dampening of channel expression levels. To offset these effects, we used an ecdysone-inducible system to co-express CaBP4 with $Ca_v1.4$ (27). Cells were co-transfected with $Ca_v1.4$ subunits as described above, but cotransfected with CaBP4 subcloned into an ecdysone-inducible expression (pIND) vector (Invitrogen; 3 μg) and pVgRXR (1 μg), which encodes a heterodimeric retinoid X receptor (RXR) and ecdysone receptor (VgEcR). After 24 h, transfected cells were treated with an ecdysone analog, Ponasterone A (10 μM; Thermo-Fisher Scientific) or 1% ethanol (control) for 8–10 h to induce CaBP4 expression.

Whole cell patch clamp recordings were performed at room temperature between 48 and 72 h after transfection. Data were obtained under voltage-clamp with an EPC-9 patch clamp amplifier operated by either Patchmaster or PULSE software (HEKA Elektronik) and analyzed with Igor Pro software (Wavemetrics). External recording solutions consisted of (in mM): Tris (140), $CaCl_2$ or $BaCl_2$ (20), and $MgCl_2$ (1). Internal pipette solution consisted of (in mM): *N*-methyl-D-glucamine (140), HEPES (10), $MgCl_2$ (2), Mg-ATP (2), and EGTA (5). The pH of external and internal recording solutions was adjusted to 7.3 with methanesulfonic acid. Pipette resistances were typically 2–4 megohms, and series resistance was compensated up to 70%. Leak subtraction was conducted using a P/4 protocol. Statistical analysis (Student's *t* test, Mann-Whitney rank sum test, or by a one-way ANOVA) was done and graphs were made with SigmaPlot (Systat Software). All averaged data

represent mean ± S.E., and result from at least 5 independent transfections.

Author Contributions—F. H. and B. W. performed experiments and analyzed data. A. L., F. H., and B. W. contributed to experimental design and writing and approval of the final manuscript.

Acknowledgments—We thank Jussara Hagen for optimizing the inducible CaBP4 expression system, the Lions Eye Bank of Oregon for providing human retinas, and the Regional Primate Center at the University of Washington for monkey retinas.

References

1. Doering, C. J., Peloquin, J. B., and McRory, J. E. (2007) The $Ca_v1.4$ calcium channel: more than meets the eye. *Channels* **1,** 3–10
2. Mansergh, F., Orton, N. C., Vessey, J. P., Lalonde, M. R., Stell, W. K., Tremblay, F., Barnes, S., Rancourt, D. E., and Bech-Hansen, N. T. (2005) Mutation of the calcium channel gene Cacna1f disrupts calcium signaling, synaptic transmission and cellular organization in mouse retina. *Hum. Mol. Genet* **14,** 3035–3046
3. Liu, X., Kerov, V., Haeseleer, F., Majumder, A., Artemyev, N., Baker, S. A., and Lee, A. (2013) Dysregulation of $Ca_v1.4$ channels disrupts the maturation of photoreceptor synaptic ribbons in congenital stationary night blindness type 2. *Channels* **7,** 514–523
4. Raven, M. A., Orton, N. C., Nassar, H., Williams, G. A., Stell, W. K., Jacobs, G. H., Bech-Hansen, N. T., and Reese, B. E. (2008) Early afferent signaling in the outer plexiform layer regulates development of horizontal cell morphology. *J. Comp. Neurol.* **506,** 745–758
5. Specht, D., Wu, S. B., Turner, P., Dearden, P., Koentgen, F., Wolfrum, U., Maw, M., Brandstätter, J. H., and tom Dieck, S. (2009) Effects of presynaptic mutations on a postsynaptic Cacna1s calcium channel colocalized with mGluR6 at mouse photoreceptor ribbon synapses. *Invest. Ophthalmol. Vis. Sci.* **50,** 505–515
6. Regus-Leidig, H., Atorf, J., Feigenspan, A., Kremers, J., Maw, M. A., and Brandstätter, J. H. (2014) Photoreceptor degeneration in two mouse models for congenital stationary night blindness type 2. *PLoS ONE* **9,** e86769
7. Bech-Hansen, N. T., Naylor, M. J., Maybaum, T. A., Pearce, W. G., Koop, B., Fishman, G. A., Mets, M., Musarella, M. A., and Boycott, K. M. (1998) Loss-of-function mutations in a calcium-channel a_1-subunit gene in Xp11.23 cause incomplete X-linked congenital stationary night blindness. *Nat. Genet.* **19,** 264–267
8. Jalkanen, R., Mäntyjärvi, M., Tobias, R., Isosomppi, J., Sankila, E. M., Alitalo, T., and Bech-Hansen, N. T. (2006) X linked cone-rod dystrophy, CORDX3, is caused by a mutation in the *CACNA1F* gene. *J. Med. Genet.* **43,** 699–704
9. Hauke, J., Schild, A., Neugebauer, A., Lappa, A., Fricke, J., Fauser, S., Rösler, S., Pannes, A., Zarrinnam, D., Altmüller, J., Motameny, S., Nürnberg, G., Nürnberg, P., Hahnen, E., and Beck, B. B. (2013) A novel large in-frame deletion within the *CACNA1F* gene associates with a cone-rod dystrophy 3-like phenotype. *PLoS ONE* **8,** e76414
10. Jalkanen, R., Bech-Hansen, N. T., Tobias, R., Sankila, E. M., Mäntyjärvi, M., Forsius, H., de la Chapelle, A., and Alitalo, T. (2007) A novel *CACNA1F* gene mutation causes Aland Island eye disease. *Invest Ophthalmol. Vis. Sci.* **48,** 2498–2502
11. Koschak, A., Reimer, D., Walter, D., Hoda, J. C., Heinzle, T., Grabner, M., and Striessnig, J. (2003) Cav1.4α1 subunits can form slowly inactivating dihydropyridine-sensitive L-type Ca^{2+} channels lacking Ca^{2+}-dependent inactivation. *J. Neurosci.* **23,** 6041–6049
12. Baumann, L., Gerstner, A., Zong, X., Biel, M., and Wahl-Schott, C. (2004) Functional characterization of the L-type Ca^{2+} channel $Ca_v1.4\alpha1$ from mouse retina. *Invest. Ophthalmol. Vis. Sci.* **45,** 708–713
13. McRory, J. E., Hamid, J., Doering, C. J., Garcia, E., Parker, R., Hamming, K., Chen, L., Hildebrand, M., Beedle, A. M., Feldcamp, L., Zamponi, G. W., and Snutch, T. P. (2004) The *CACNA1F* gene encodes an L-type calcium channel with unique biophysical properties and tissue distribution. *J. Neurosci.* **24,** 1707–1718
14. Witkovsky, P., Schmitz, Y., Akopian, A., Krizaj, D., and Tranchina, D. (1997) Gain of rod to horizontal cell synaptic transfer: relation to glutamate release and a dihydropyridine-sensitive calcium current. *J. Neurosci.* **17,** 7297–7306
15. Thoreson, W. B., Rabl, K., Townes-Anderson, E., and Heidelberger, R. (2004) A highly Ca^{2+}-sensitive pool of vesicles contributes to linearity at the rod photoreceptor ribbon synapse. *Neuron* **42,** 595–605
16. Ben-Johny, M., and Yue, D. T. (2014) Calmodulin regulation (calmodulation) of voltage-gated calcium channels. *J. Gen. Physiol.* **143,** 679–692
17. Christel, C., and Lee, A. (2012) Ca^{2+}-dependent modulation of voltage-gated Ca^{2+} channels. *Biochim. Biophys. Acta* **1820,** 1243–1252
18. Hoda, J. C., Zaghetto, F., Singh, A., Koschak, A., and Striessnig, J. (2006) Effects of congenital stationary night blindness type 2 mutations R508Q and L1364H on Cav1.4 L-type Ca^{2+} channel function and expression. *J. Neurochem.* **96,** 1648–1658
19. Wahl-Schott, C., Baumann, L., Cuny, H., Eckert, C., Griessmeier, K., and Biel, M. (2006) Switching off calcium-dependent inactivation in L-type calcium channels by an autoinhibitory domain. *Proc. Natl. Acad. Sci. U.S.A.* **103,** 15657–15662
20. Griessmeier, K., Cuny, H., Rötzer, K., Griesbeck, O., Harz, H., Biel, M., and Wahl-Schott, C. (2009) Calmodulin is a functional regulator of $Ca_v1.4$ L-type Ca^{2+} channels. *J. Biol. Chem.* **284,** 29809–29816
21. Strom, T. M., Nyakatura, G., Apfelstedt-Sylla, E., Hellebrand, H., Lorenz, B., Weber, B. H., Wutz, K., Gutwillinger, N., Rüther, K., Drescher, B., Sauer, C., Zrenner, E., Meitinger, T., Rosenthal, A., and Meindl, A. (1998) An L-type calcium-channel gene mutated in incomplete X-linked congenital stationary night blindness. *Nat. Genet.* **19,** 260–263
22. Singh, A., Hamedinger, D., Hoda, J. C., Gebhart, M., Koschak, A., Romanin, C., and Striessnig, J. (2006) C-terminal modulator controls Ca^{2+}-dependent gating of $Ca_v1.4$ L-type Ca^{2+} channels. *Nat. Neurosci.* **9,** 1108–1116
23. Tan, G. M., Yu, D., Wang, J., and Soong, T. W. (2012) Alternative splicing at C terminus of $Ca_v1.4$ calcium channel modulates calcium-dependent inactivation, activation potential, and current density. *J. Biol. Chem.* **287,** 832–847
24. Haeseleer, F., Sokal, I., Verlinde, C. L., Erdjument-Bromage, H., Tempst, P., Pronin, A. N., Benovic, J. L., Fariss, R. N., and Palczewski, K. (2000) Five members of a novel Ca^{2+}-binding protein (CABP) subfamily with similarity to calmodulin. *J. Biol. Chem.* **275,** 1247–1260
25. Cui, G., Meyer, A. C., Calin-Jageman, I., Neef, J., Haeseleer, F., Moser, T., and Lee, A. (2007) Ca^{2+}-binding proteins tune Ca^{2+}-feedback to $Ca_v1.3$ channels in auditory hair cells. *J. Physiol.* **585,** 791–803
26. Zhou, H., Kim, S. A., Kirk, E. A., Tippens, A. L., Sun, H., Haeseleer, F., and Lee, A. (2004) Ca^{2+}-binding protein-1 facilitates and forms a postsynaptic complex with $Ca_v1.2$ (L-type) Ca^{2+} channels. *J. Neurosci.* **24,** 4698–4708
27. Yang, P. S., Alseikhan, B. A., Hiel, H., Grant, L., Mori, M. X., Yang, W., Fuchs, P. A., and Yue, D. T. (2006) Switching of Ca^{2+}-dependent inactivation of $Ca_v1.3$ channels by calcium binding proteins of auditory hair cells. *J. Neurosci.* **26,** 10677–10689
28. Oz, S., Benmocha, A., Sasson, Y., Sachyani, D., Almagor, L., Lee, A., Hirsch, J. A., and Dascal, N. (2013) Competitive and non-competitive regulation of calcium-dependent inactivation in $Ca_V1.2$ L-type Ca^{2+} channels by calmodulin and Ca^{2+}-binding protein 1. *J. Biol. Chem.* **288,** 12680–12691
29. Findeisen, F., Rumpf, C. H., and Minor, D. L., Jr. (2013) Apo states of calmodulin and CaBP1 control Ca_V1 voltage-gated calcium channel function through direct competition for the IQ domain. *J. Mol. Biol.* **425,** 3217–3234
30. Yang, P. S., Johny, M. B., and Yue, D. T. (2014) Allostery in Ca^{2+} channel modulation by calcium-binding proteins. *Nat. Chem. Biol.* **10,** 231–238
31. Haeseleer, F., Imanishi, Y., Maeda, T., Possin, D. E., Maeda, A., Lee, A., Rieke, F., and Palczewski, K. (2004) Essential role of Ca^{2+}-binding protein 4, a $Ca_v1.4$ channel regulator, in photoreceptor synaptic function. *Nat. Neurosci.* **7,** 1079–1087
32. Shaltiel, L., Paparizos, C., Fenske, S., Hassan, S., Gruner, C., Rötzer, K., Biel, M., and Wahl-Schott, C. A. (2012) Complex regulation of voltage-depen-

dent activation and inactivation properties of retinal voltage-gated $Ca_v1.4$ L-type Ca^{2+} channels by Ca^{2+}-binding protein 4 (CaBP4). *J. Biol. Chem.* **287,** 36312–36321
33. Corey, D. P., Dubinsky, J. M., and Schwartz, E. A. (1984) The calcium current in inner segments of rods from the salamander (*Ambystoma tigrinum*) retina. *J. Physiol.* **354,** 557–575
34. Liu, X., Yang, P. S., Yang, W., and Yue, D. T. (2010) Enzyme-inhibitor-like tuning of Ca^{2+} channel connectivity with calmodulin. *Nature* **463,** 968–972
35. Dolphin, A. C. (2013) The $\alpha_2\delta$ subunits of voltage-gated calcium channels. *Biochim. Biophys. Acta* **1828,** 1541–1549
36. Buraei, Z., and Yang, J. (2010) The β subunit of voltage-gated Ca^{2+} channels. *Physiol. Rev.* **90,** 1461–1506
37. Ball, S. L., Powers, P. A., Shin, H. S., Morgans, C. W., Peachey, N. S., and Gregg, R. G. (2002) Role of the β_2 subunit of voltage-dependent calcium channels in the retinal outer plexiform layer. *Invest. Ophthalmol. Vis. Sci.* **43,** 1595–1603
38. Wycisk, K. A., Budde, B., Feil, S., Skosyrski, S., Buzzi, F., Neidhardt, J., Glaus, E., Nürnberg, P., Ruether, K., and Berger, W. (2006) Structural and functional abnormalities of retinal ribbon synapses due to Cacna2d4 mutation. *Invest. Ophthalmol. Vis. Sci.* **47,** 3523–3530
39. Katiyar, R., Weissgerber, P., Roth, E., Dörr, J., Sothilingam, V., Garcia Garrido, M., Beck, S. C., Seeliger, M. W., Beck, A., Schmitz, F., and Flockerzi, V. (2015) Influence of the β2-subunit of L-type voltage-gated Cav channels on the structural and functional development of photoreceptor ribbon synapses. *Invest. Ophthalmol. Vis. Sci.* **56,** 2312–2324
40. Lee, A., Wang, S., Williams, B., Hagen, J., Scheetz, T. E., and Haeseleer, F. (2015) Characterization of Cav1.4 complexes ($\alpha_1$1.4, β_1, and $\alpha_2\delta_4$) in HEK293T cells and in the retina. *J. Biol. Chem.* **290,** 1505–1521
41. Livak, K. J., and Schmittgen, T. D. (2001) Analysis of relative gene expression data using real-time quantitative PCR and the $2^{-\Delta\Delta Ct}$ method. *Methods* **25,** 402–408
42. Calin-Jageman, I., Yu, K., Hall, R. A., Mei, L., and Lee, A. (2007) Erbin enhances voltage-dependent facilitation of $Ca_v1.3$ Ca^{2+} channels through relief of an autoinhibitory domain in the $Ca_v1.3$ α_1 subunit. *J. Neurosci.* **27,** 1374–1385
43. Singh, A., Gebhart, M., Fritsch, R., Sinnegger-Brauns, M. J., Poggiani, C., Hoda, J. C., Engel, J., Romanin, C., Striessnig, J., and Koschak, A. (2008) Modulation of voltage- and Ca^{2+}-dependent gating of $Ca_V1.3$ L-type calcium channels by alternative splicing of a C-terminal regulatory domain. *J. Biol. Chem.* **283,** 20733–20744
44. Tan, B. Z., Jiang, F., Tan, M. Y., Yu, D., Huang, H., Shen, Y., and Soong, T. W. (2011) Functional characterization of alternative splicing in the C terminus of L-type $Ca_V1.3$ channels. *J. Biol. Chem.* **286,** 42725–42735
45. Hulme, J. T., Yarov-Yarovoy, V., Lin, T. W., Scheuer, T., and Catterall, W. A. (2006) Autoinhibitory control of the $Ca_V1.2$ channel by its proteolytically processed distal C-terminal domain. *J. Physiol.* **576,** 87–102
46. Scharinger, A., Eckrich, S., Vandael, D. H., Schönig, K., Koschak, A., Hecker, D., Kaur, G., Lee, A., Sah, A., Bartsch, D., Benedetti, B., Lieb, A., Schick, B., Singewald, N., Sinnegger-Brauns, M. J., Carbone, E., Engel, J., and Striessnig, J. (2015) Cell-type-specific tuning of $Ca_v1.3$ Ca^{2+}-channels by a C-terminal automodulatory domain. *Front. Cell Neurosci.* **9,** 309
47. Lieb, A., Ortner, N., and Striessnig, J. (2014) C-terminal modulatory domain controls coupling of voltage-sensing to pore opening in $Ca_v1.3$ L-type Ca^{2+} channels. *Biophys. J.* **106,** 1467–1475
48. Catterall, W. A. (2010) Ion channel voltage sensors: structure, function, and pathophysiology. *Neuron* **67,** 915–928
49. Hardie, J., and Lee, A. (2016) Decalmodulation of Cav1 channels by CaBPs. *Channels* **10,** 33–37
50. Ball, S. L., McEnery, M. W., Yunker, A. M., Shin, H. S., and Gregg, R. G. (2011) Distribution of voltage gated calcium channel β subunits in the mouse retina. *Brain Res.* **1412,** 1–8
51. Frankenhaeuser, B., and Hodgkin, A. L. (1957) The action of calcium on the electrical properties of squid axons. *J. Physiol.* **137,** 218–244
52. Kostyuk, P., Mironov, S. L., Doroshenko, P. A., and Ponomarev, V. N. (1982) Surface charges on the outer side of mollusc neuron membrane. *J. Membr. Biol.* **70,** 171–179
53. Berntson, A., Smith, R. G., and Taylor, W. R. (2004) Transmission of single photon signals through a binary synapse in the mammalian retina. *Vis. Neurosci.* **21,** 693–702
54. Field, G. D., and Rieke, F. (2002) Nonlinear signal transfer from mouse rods to bipolar cells and implications for visual sensitivity. *Neuron* **34,** 773–785
55. Lee, A., Fakler, B., Kaczmarek, L. K., and Isom, L. L. (2014) More than a pore: ion channel signaling complexes. *J. Neurosci.* **34,** 15159–15169
56. Lipscombe, D., Allen, S. E., and Toro, C. P. (2013) Control of neuronal voltage-gated calcium ion channels from RNA to protein. *Trends Neurosci.* **36,** 598–609 .